

Mapping 1+1-dimensional black hole thermodynamics to finite volume effects

Jean Alexandre¹, Drew Backhouse¹, Eleni-Alexandra Kontou², Diego Pardo Santos^{2*} and Silvia Pla^{1,3}

¹ Department of Physics, King's College London, Strand, London, WC2R 2LS, United Kingdom

² Department of Mathematics, King's College London, Strand, London WC2R 2LS, United Kingdom

³ Physik-Department, Technische Universität München, James-Franck-Str., 85748 Garching, Germany

* diego.pardo@kcl.ac.uk

Abstract

Both black hole thermodynamics and finite volume effects in quantum field theory violate the null energy condition. Motivated by this, we compare thermodynamic features between two 1+1-dimensional systems: (i) a scalar field confined to a periodic spatial interval of length a and tunneling between two degenerate vacua; (ii) a dilatonic black hole at temperature T in the presence of matter fields. If we identify $a \propto T^{-1}$, we find similar thermodynamic behaviour, which suggests some deeper connection arising from the presence of non-trivial boundary conditions in both systems.

Copyright attribution to authors.

This work is a submission to SciPost Physics.

License information to appear upon publication.

Publication information to appear upon publication.

Received Date

Accepted Date

Published Date

1

2 Contents

3	1 Introduction	2
4	2 Finite size effects in 1+1 dimensional flat spacetime	4
5	2.1 Convexity from tunnelling	4
6	2.2 Tunneling and the Casimir effect	5
7	2.2.1 Semi-classical approximation and true vacuum	5
8	2.2.2 Static saddle points	6
9	2.2.3 Time-dependent saddle points	6
10	2.2.4 Partition function	7
11	2.3 Null Energy Condition	8
12	2.4 Entropy	10
13	3 Black holes in 1+1 dilaton gravity	11
14	3.1 Introduction to dilaton gravity	11
15	3.2 Adding quantum matter: static black holes	13
16	3.3 Without backreaction, the CGHS model	15

17	3.3.1 Null energy condition	15
18	3.3.2 Entropy and thermodynamics	16
19	3.4 With backreaction, the BPP model	17
20	3.4.1 Null energy condition	18
21	3.4.2 Entropy and thermodynamics	18
22	4 Comparison	19
23	5 Conclusions	20
24	A Casimir effect for static saddle points	21
25	A.1 Zero temperature	22
26	A.2 Finite-temperature corrections	22
27	References	23
28		
29		

30 1 Introduction

31 One of the seminal results in semi-classical gravity is Hawking radiation, and subsequent black
 32 hole evaporation [1]. Part of its importance is that it shows a clear quantum effect in a regime
 33 where the curvature is small (the black hole horizon) and thus it can be treated classically.
 34 An important consequence of Hawking radiation is the violation of the null energy condition
 35 (NEC) around the black hole horizon.

36 The NEC is part of the classical energy conditions which are what we call *pointwise*: they
 37 restrict some contraction of the stress tensor at every spacetime point (see [2] and [3] for
 38 reviews). The NEC is the weakest of them and it is written as

$$T_{\mu\nu}\ell^\mu\ell^\nu \geq 0, \quad (1)$$

39 where $T_{\mu\nu}$ is the stress-energy tensor and ℓ^μ a null vector field. The NEC is obeyed by most
 40 classical fields¹ and it is often considered an important property of physical matter. Its ge-
 41 ometric form, obtained by the use of the Einstein equation, is called the null convergence
 42 condition and it implies that a non-rotating null geodesic congruence locally converges. It was
 43 famously used in Penrose's singularity theorem [6], Hawking's black hole area theorem [7]
 44 and other classical relativity results. If the stress-energy tensor has the form of a perfect fluid,
 45 $T_{\mu\nu} = (\rho + p)v^\mu v^\nu + pg^{\mu\nu}$, where ρ is the energy density, p the pressure and v^μ is the fluid's
 46 unit four-velocity vector field, the NEC becomes

$$\rho + p \geq 0. \quad (2)$$

47 The NEC, as is the case for all pointwise energy conditions, is violated in the context of semi-
 48 classical gravity; with the most prominent case being the Hawking radiation. More generally,
 49 quantum field theories (QFTs) obeying some reasonable axioms always have states that admit
 50 negative energy as shown by Epstein, Glaser and Jaffe in the 1960's [8].

51 Interestingly, the NEC is violated in a different setting, involving finite volume effects in
 52 scalar QFT. A finite volume in QFT implies two fundamental features: quantisation of momen-
 53 tum and tunnelling between multiple vacua. The first feature is at the origin of the Casimir

¹It is however violated by scalars with non-minimal coupling to gravity [4, 5].

System	NEC violation	Entropy rate
Tunneling in 1+1 flat spacetime	$-\frac{\pi}{3a^2}$	$\frac{1}{2} - \frac{2m}{3}a$
1+1 Dilatonic Black Holes	$-\frac{N\pi^2}{12}T^2$	$-\frac{N}{12} - \frac{M}{\pi T}$

Table 1: Summary of results comparing the two thermodynamical systems, for NEC violation and the rate of change in entropy: (i) Tunneling in 1+1 flat spacetime (cf. eqs. (31) and (95)); (ii) 1+1 Dilatonic Black Holes (cf. eqs. (68) and (96)). N is the number of massless scalar fields.

54 effect (see [9] for a review), which is known to induce NEC violation. As shown more recently
 55 and reviewed in the next section, the second feature also leads to NEC violation, in relation to
 56 convexity of the effective potential [10–14]. For both the Casimir effect and tunnelling, NEC
 57 violation arises from a ground state energy which is not extensive, i.e. not simply proportional
 58 to the size of the system.

59 We investigate the possibility of a correspondence between these two sources of NEC vio-
 60 lation. In particular: (i) a scalar field confined to a periodic spatial interval of length a and
 61 tunnelling between two degenerate vacua in the limit of zero temperature; (ii) a dilatonic
 62 black hole at temperature T in the presence of matter fields in an infinite spatial volume.

63 For simplicity, the particular systems we are considering are both 1+1-dimensional.² The
 64 motivation is to find common features between two non-trivial thermodynamical systems due
 65 to quantum effects. Our main results are summarised in table 1, in the regime $ma \propto M/T \lesssim 1$,
 66 where m, a are respectively the mass and length scales in the tunnelling description, and M, T
 67 are respectively the mass and temperature of the dilatonic black hole (which are independent
 68 parameters). The two systems are thermodynamically similar under the matching condition
 69 of $a \propto 1/T$, suggesting a mapping between finite size and finite temperature. It is important
 70 to note that this analogy cannot be attributed to dimensional considerations though, since
 71 several length/mass scales are present in both models.

72 We stress here that this work does not establish rigorously a duality between the two sys-
 73 tems, as one could hope from the AdS/CFT correspondence for example. The aim of this
 74 approach is to put forward a complementary study, which could provide a different angle on
 75 black hole thermodynamics, based on an analogy with a simpler system in flat spacetime. Our
 76 strategy is to first derive new properties, both for the confined scalar field and the dilatonic
 77 black hole, but independently. The resulting mapping $T \leftrightarrow a^{-1}$ we then find is not trivial,
 78 and suggests that further studies could be made, requiring a more systematic formalism. Our
 79 results are therefore preliminary, but promising for a new and original mapping

80 In section 2 we calculate the free energy for the ground state resulting from the scalar
 81 field tunnelling between degenerate minima. We explain why in one space dimension, the
 82 Casimir and tunnelling effects are of the same order of magnitude. In the limit of vanishing
 83 temperature, NEC violation can be decomposed as the sum of two contributions: one from the
 84 Casimir effect and one from tunnelling. We show that the latter is actually more important
 85 than the former if $ma \gtrsim 1$, which is a new feature with relevance potentially going beyond the
 86 present study.

87 Section 3 presents the derivation of the thermodynamical properties of the dilatonic black
 88 hole in the presence of non-self-interacting matter fields. A detailed explanation is given for

²Other studies of finite volume QFT effects in 1+1 dimensional spacetime can be found in [15].

89 the role of the environment regarding the entropy of the system once backreaction of the
90 matter fields on the background metric is taken into account.

91 In section 4 we compare the two studies and we find that the relation $a \propto T^{-1}$ provides a
92 mapping between the two systems.

93 Tunnelling at finite temperature is described with a Euclidean metric whereas the metric
94 sign convention for the black hole description is $(-, +)$. Natural units of $\hbar = c = 1$ are used
95 throughout.

96 2 Finite size effects in 1+1 dimensional flat spacetime

97 We consider a massive self-interacting real scalar field theory defined on a one-dimensional
98 periodic interval $x \in [0, a]$ at a temperature $T \equiv 1/\beta$ with a corresponding Euclidean action

$$I = \frac{1}{2} \int_0^\beta d\tau \int_0^a dx \left((\dot{\phi})^2 + (\phi')^2 + \frac{m^2}{4} (\phi^2 - 1)^2 \right), \quad (3)$$

99 where m is the mass scale of the theory. Starting from this we study the thermodynamics of
100 the true vacuum of the effective theory.

101 2.1 Convexity from tunnelling

102 It is known that the one-Particle-Irreducible (1PI) effective potential is necessarily convex if
103 one takes several vacua into account [16–25]. Focusing on two degenerate vacua at $\pm v$, the
104 dynamics of this feature relies on tunnelling between these vacua [10], which restores sym-
105 metry and induces a true ground state corresponding to a vanishing field expectation value
106 $\langle \phi \rangle = 0$ (see figure 1). Equivalently, by symmetry of the bare potential, the true vacuum
107 corresponds to a vanishing source $j = 0$, and

$$\langle \phi \rangle \equiv - \frac{1}{Z[j]} \left. \frac{\delta Z[j]}{\delta j} \right|_{j=0} = 0, \quad (4)$$

108 where $Z[j]$ is the partition function. The picture described here can be interpreted as back-
109 reaction: the double-well bare potential allows quantum fluctuations to tunnel between the
110 minima, which in turns modifies the vacuum structure by imposing convexity. The resulting
111 symmetric vacuum corresponds then to a non-perturbative process, which can be described by
112 the semi-classical approximation for $Z[j]$, as explained below.

113 Symmetry restoration is possible in a finite volume only, though, since an infinite volume
114 implies Spontaneous Symmetry Breaking instead. But a finite volume requires a discrete set
115 of momenta for quantum fluctuations and, as we show in this article, in the limit of vanishing
116 temperature, finite-size effects can be decomposed as the sum of two contributions: (i) dis-
117 cretisation of momentum for quantum fluctuations, that we will refer to as the Casimir effect;
118 (ii) symmetry restoration due to tunnelling, that we will refer to as the tunnelling effect.

119 Allowing tunnelling between two degenerate vacua, the 1PI effective potential induced by
120 a dilute gas of instantons was calculated in [11], based on an expansion in $\langle \phi \rangle$ to the quadratic
121 order. This result explicitly shows a convex effective potential, with a positive mass term and
122 a true vacuum at $\langle \phi \rangle = 0$. Focusing on this true vacuum, the complete one-loop quantisation
123 of the dilute gas with discrete momentum is calculated in [14] for a 3-torus, providing the full
124 picture of the interplay between Casimir and tunnelling effects.

125 These calculations were done in 3+1 dimensions though, and we consider here the 1+1
126 dimensional case, where both effects are comparable. Indeed, for a finite length a and a mass

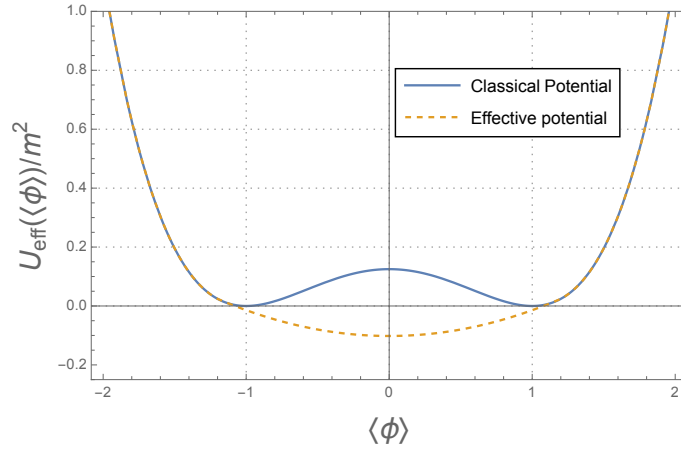


Figure 1: The classical potential (solid blue) and effective potential (dashed orange) in a finite spatial volume. The effective potential is necessarily convex due to tunneling between the two degenerate vacua, restoring symmetry.

127 scale m , the instanton action is of the order ma , leading for $ma \gg 1$ to a suppression of the
 128 tunnelling effect of the order $\exp(-ma)$, similarly to what happens in the Casimir effect.

129 As we show in this section, one feature of convexity obtained from quantum fluctuations is
 130 NEC violation in the true ground state. If we allowed the system to evolve freely, this violation
 131 would imply an increase in the length a , similarly to spacetime expansion due to tunnelling-
 132 induced NEC violation, as described in [12, 13] (see for example [26, 27] for reviews of NEC
 133 violation in the context of Cosmology). In the present work, we do not take into account
 134 spacetime dynamics though, and we stick to static QFT. This implies that some external system
 135 fixes the length a , which requires some energy. As a consequence, although the confined scalar
 136 field violates the NEC, the Averaged NEC is not violated, which can be seen by integrating the
 137 NEC along a null geodesic going through the confining walls [28–30].

138 The main part of this section focuses on the zero-temperature case, since thermal effects
 139 tend to restore the NEC. Nevertheless we start the calculations at finite temperature β^{-1} , and
 140 consider then the limit $\beta \rightarrow \infty$.

141 2.2 Tunneling and the Casimir effect

142 2.2.1 Semi-classical approximation and true vacuum

143 Defining the dimensionless variables

$$t \equiv m\tau \quad \text{and} \quad r \equiv mx, \quad (5)$$

144 the action of eq. (3) becomes

$$I = \frac{1}{2} \int_0^{m\beta} dt \int_0^{ma} dr \left((\dot{\phi})^2 + (\phi')^2 + \frac{1}{4}(\phi^2 - 1)^2 \right), \quad (6)$$

145 where dots and primes now represent derivatives in t and r respectively. One can see that this
 146 action depends on the two dimensionless parameters ma and $m\beta$, and is invariant under the
 147 simultaneous rescaling

$$a \rightarrow \lambda a, \quad \beta \rightarrow \lambda \beta, \quad m \rightarrow m/\lambda, \quad (7)$$

148 and the quantum theory should also respect this symmetry, as we confirm in what follows. The
 149 equation of motion (EoM) with solutions ϕ_i is

$$\ddot{\phi}_i + \frac{1}{2}(\phi_i - \phi_i^3) = 0, \quad (8)$$

150 where in this work we consider only Euclidean-time-dependent and homogeneous configura-
 151 tions ϕ_i , since vacuum bubbles forming from degenerate vacua would have an infinite ra-
 152 dius [31, 32]. There are several solutions to the classical EoM (8), each to be studied in
 153 following subsections.

154 For a vanishing source $j = 0$ and in the semi-classical approximation, the partition function
 155 $Z[0] \equiv Z$ can be approximated as a sum of path integrals over regions in field space around
 156 the action minimising saddle points φ_i via the field decomposition $\varphi = \varphi_i + \psi$, integrating
 157 over fluctuations ψ . This assumes that the fluctuations do not overlap, and the one-loop
 158 approximation for the fluctuation factors leads to

$$\begin{aligned} Z &= \int \mathcal{D}[\phi] \exp(-I[\phi]) \\ &\simeq \sum_i \int \mathcal{D}[\psi] \exp(-I[\varphi_i + \psi]) \\ &= \sum_i (\det(\delta^2 I[\phi_i]))^{-1/2} \exp(-I[\phi_i]) \\ &\equiv \sum_i \exp(-W[\phi_i]), \end{aligned} \quad (9)$$

159 where the individual connected graph generating functionals are

$$W[\phi_i] \equiv I[\phi_i] + \frac{1}{2} \text{Tr} \{ \ln(\delta^2 I[\phi_i]) \}. \quad (10)$$

160 2.2.2 Static saddle points

161 There are two static saddle points in the present model, $\phi_s = \pm 1$. The corresponding indi-
 162 vidual connected graph generating functionals (10) can be evaluated using known methods
 163 developed for the study of the thermal Casimir effect on a 1D periodic interval [9]. The steps
 164 are outlined in appendix A and lead to

$$W_{\text{stat}}(a, \beta) \equiv W[\phi_s] = a\beta\Lambda^2 - \frac{m^2 a\beta}{\pi} \int_1^\infty du \frac{\sqrt{u^2 - 1}}{e^{mau} - 1} + \sum_{n \in \mathbb{Z}} \ln(1 - e^{-\beta\omega_n}), \quad (11)$$

165 where Λ^2 is an ultraviolet cutoff, corresponding to the vacuum energy of unbounded space,
 166 and the quantised frequencies/wave vectors are

$$\omega_n = \sqrt{m^2 + k_n^2}, \quad k_n = \frac{2\pi n}{a}. \quad (12)$$

167 We note here that quantum corrections indeed depend on a, β, m through the products ma
 168 and $m\beta$ only.

169 2.2.3 Time-dependent saddle points

170 The fundamental time-dependent saddle point is the (anti-)instanton relating the two vacua
 171 of the bare potential

$$\phi_{\text{inst}}(t) = (\pm) \tanh\left(\frac{t - t_1}{2}\right), \quad (13)$$

172 where t_1 is the time of the jump. At a finite temperature, field configurations are periodic in
 173 Euclidean time and hence instantons and anti-instantons can only exist in pairs. Such field

174 configurations are well approximated by a product of individual (anti-)instanton configura-
175 tions

$$\phi_{n\text{-pair}}(\tau) \simeq \prod_{j=1}^{2n} (-1)^j \tanh\left(\frac{t-t_j}{2}\right), \quad (14)$$

176 provided that the jumps at t_i and t_j are sufficiently distant ($|t_i - t_j| \gg 1$). The factor -1
177 ensures that an instanton is always followed by an anti-instanton and the product is taken to
178 $2n$ to enforce periodicity in Euclidean time. In the limit of small temperature, $m\beta \gg 1$, a
179 large amount of instanton/anti-instanton pairs is allowed and we assume in what follows the
180 instanton dilute gas approximation [33], where the width of each jump is negligible compared
181 to $m\beta$. Also, (anti-)instantons are far enough from each other for them to keep their shape,
182 which for n pairs leads to the total action

$$I_{n\text{-pairs}} \simeq 2nI_{\text{inst}}, \quad (15)$$

183 where the action for one (anti-)instanton is

$$I_{\text{inst}} \equiv I[\phi_{\text{inst}}] = \frac{2ma}{3}. \quad (16)$$

184 The fluctuation factor for n instanton/anti-instanton pairs can then be approximated by the
185 product of fluctuation factors for each static saddle point evaluated over half the total Eu-
186 clidean time interval $\beta/2$, times the fluctuation factors for each instanton jump. The corre-
187 sponding connected graph generating functional is then

$$W_{n\text{-pairs}} \equiv W[\phi_{n\text{-pair}}] \simeq 2W_{\text{stat}}(a, \beta/2) + 2nW_{\text{jump}}, \quad (17)$$

188 where we know from tunnelling in Quantum Mechanics [33] that

$$W_{\text{jump}} \equiv I_{\text{inst}} - \frac{1}{2} \ln\left(\frac{6I_{\text{inst}}}{\pi}\right). \quad (18)$$

189 We note that the expression for W_{jump} takes into account time-dependent quantum fluctuations
190 over the instantons, and it neglects the space-dependence of these fluctuations. However, it
191 was shown in [14] that the main contribution of the instanton jump comes from the zero-
192 modes, validating the approximation made here.

193 2.2.4 Partition function

194 Assuming the semi-classical approximation and a dilute gas of instantons/anti-instantons, the
195 partition function can be expressed as a sum over all the possible n -pair configurations

$$Z \simeq 2 \exp(-W_{\text{stat}}(a, \beta)) + 2 \sum_{n=1}^{\infty} \left(\prod_{i=1}^{2n} \int_{t_{i-1}}^{m\beta} dt_i \right) \exp(-2W_{\text{stat}}(a, \beta/2) - 2nW_{\text{jump}}). \quad (19)$$

196 The first term in the right-hand side corresponds to the two static saddle points. In the second
197 term the product of integrals accounts for the invariance of the total action $I_{n\text{-pairs}}$ under the
198 translations of each successive instanton jump over the remaining dimensionless Euclidean
199 time interval $t \in [t_i, m\beta]$, defining $t_0 \equiv 0$ since the first instanton can exist over the whole
200 interval. This invariance under translation of the jumps corresponds to the zero modes of the
201 fluctuation factors for each n -pair configuration. The factor 2 takes into account the instanton
202 configurations starting and ending at either $+1$ or -1 . Using the known result [31]

$$\prod_{i=1}^{2n} \int_{t_{i-1}}^{m\beta} dt_i = \frac{(m\beta)^{2n}}{(2n)!}, \quad (20)$$

203 the partition function (19) can be expressed as

$$Z \simeq 2 \exp(-W_{\text{stat}}(a, \beta)) + 2 \exp(-2W_{\text{stat}}(a, \beta/2)) \sum_{n=1}^{\infty} \frac{\bar{N}^{2n}}{(2n)!}, \quad (21)$$

204 where

$$\bar{N} \equiv m\beta \sqrt{\frac{6J_{\text{inst}}}{\pi}} e^{-I_{\text{inst}}} = 2m\beta \sqrt{\frac{ma}{\pi}} \exp\left(-\frac{2ma}{3}\right), \quad (22)$$

205 with $\bar{N}/2$ corresponding to the average number of instanton/anti-instanton pairs over the
206 whole Euclidean time β [10]. In the small temperature limit ($m\beta \gg 1$) the last term in W_{stat}
207 (11) can be neglected, such that it can be taken as linear in β

$$W_{\text{stat}}(a, \beta) \simeq 2W_{\text{stat}}(a, \beta/2), \quad (23)$$

208 and the partition function (21) becomes ³

$$Z \simeq 2 \exp(-2W_{\text{stat}}(a, \beta/2)) \sum_{n=0}^{\infty} \frac{\bar{N}^{2n}}{(2n)!} = 2 \exp(-2W_{\text{stat}}(a, \beta/2)) \cosh(\bar{N}). \quad (24)$$

209 Finally, in the limit $m\beta \gg 1$ for finite ma (such that $\bar{N} \gg 1$) the total free energy is

$$F_{\text{true}} \equiv -T \ln(Z) \simeq 2TW_{\text{stat}}(a, \beta/2) - T\bar{N}, \quad (25)$$

210 and corresponds to the sum of the usual free-field Casimir contribution $2TW_{\text{stat}}(a, \beta/2)$ and
211 the tunneling contribution $-T\bar{N}$.

212 2.3 Null Energy Condition

213 We show here that the true ground state of the system we consider violates the NEC, as a
214 consequence of the true vacuum energy not being extensive: the free energy (25) is not simply
215 proportional to a .

216 We assume here that the dilute instanton gas described by the partition function (24) may
217 be treated as a perfect fluid, such that the resulting null energy condition reduces to the simpler
218 form (2). The thermodynamic energy density and pressure are then defined as

$$\rho \equiv \frac{1}{a} \left(F_{\text{true}} + \beta \frac{\partial F_{\text{true}}}{\partial \beta} \right), \quad (26)$$

$$p \equiv -\frac{\partial F_{\text{true}}}{\partial a}. \quad (27)$$

219 Here we show that the NEC is violated by the finite volume effects we consider.

220 The sum $\rho + p$ may be evaluated from the free energy (25) and satisfies

$$\begin{aligned} \frac{\rho + p}{m^2} &= -\frac{ma}{\pi} \int_1^{\infty} du \frac{ue^{mau} \sqrt{u^2 - 1}}{(e^{mau} - 1)^2} - \frac{4ma + 3}{3\sqrt{\pi ma}} \exp\left(-\frac{2ma}{3}\right) \\ &+ \sum_{n \in \mathbb{Z}} \frac{m^2 a^2 + 8n^2 \pi^2}{m^2 a^3 \omega_n} (e^{\beta \omega_n / 2} - 1)^{-1}, \end{aligned} \quad (28)$$

221 where we can identify the following terms:

³The approximation (23) is applied to the static saddle point contribution, and not to the instanton contribution, since it is sub-dominant at low temperatures.

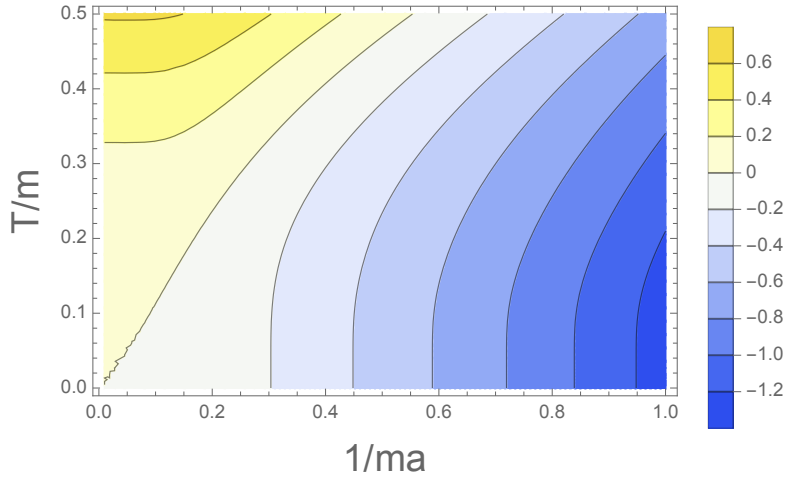


Figure 2: Numerical plot of $(\rho + p)/m^2$ (28) for inverse dimensionless length $1/ma$ with finite temperature corrections. At zero temperature, NEC violation increases as the spatial interval reduces, corresponding to an increased tunneling rate, and approaches zero in the limit of infinite spatial length where tunneling is completely suppressed. For a given length scale, finite temperature effects increase $\rho + p$ and can lead to NEC satisfaction at large length scales.

- 222 (i) the first term (integral over t) corresponds to the known Casimir effect, obtained for a
 223 free field, with a negative contribution;
- 224 (ii) the second term corresponds to tunnelling arising from degenerate vacua, with a nega-
 225 tive contribution;
- 226 (iii) the third term (sum over Matsubara modes) corresponds to finite temperature effects
 227 providing a positive contribution, and becomes the usual contribution from black body
 228 radiation ($\propto T^2$) in the massless and infinite length limit.

229 The expression (28) is plotted in figure 2 as a function of inverse dimensionless spatial length
 230 $1/ma$ with finite temperature corrections.

231 Thermal effects decrease exponentially for small temperatures: for $m\beta \gg 1$ we have

$$\sum_{n \in \mathbb{Z}} \frac{m^2 a^2 + 8n^2 \pi^2}{m^2 a^3 \omega_n} (e^{\beta \omega_n/2} - 1)^{-1} \simeq \frac{e^{-m\beta/2}}{am}, \quad (29)$$

232 and in what follows we take the limit $\beta \rightarrow \infty$, in order to focus on NEC violating finite-length
 233 effects. It is then interesting to look at two asymptotic regimes for the length a :

234 – $ma \gg 1$ In this case we have

$$\frac{\rho + p}{m^2} \approx -\frac{e^{-am}}{\sqrt{2\pi am}} - \frac{4}{3} \sqrt{\frac{am}{\pi}} e^{-2ma/3}, \quad (30)$$

235 and we can see that tunnelling effects are more important than the free-field Casimir
 236 effect;

237 – $ma \lesssim 1$ In this case we have

$$\frac{\rho + p}{m^2} \approx -\frac{\pi}{3(am)^2}, \quad (31)$$

238 where tunnelling is negligible and the result is identical to the one obtained for a massless
 239 free field [9].

240 2.4 Entropy

241 At zero temperature the classical thermal entropy vanishes, which can be seen with

$$\mathcal{S}_{\text{classical}} = -\lim_{T \rightarrow 0} \frac{\partial F_{\text{true}}}{\partial T} = 0. \quad (32)$$

242 There is a quantum contribution left though, which can be interpreted as the entropy for
 243 the dilute gas of instantons/anti-instantons which relate the two vacua. Taking into account
 244 the instanton fluctuation factors described above, the probability of having n instanton/anti-
 245 instanton pairs may be read off from the partition function Z

$$p_n = \frac{2}{Z} \frac{(\bar{N})^{2n}}{(2n)!} e^{-2W_{\text{stat}}(\beta/2)} = \frac{1}{\cosh(\bar{N})} \frac{(\bar{N})^{2n}}{(2n)!}, \quad (33)$$

246 where Z , \bar{N} and W_{stat} are given by eqs. (24), (22) and (11) respectively. The entropy of
 247 the dilute gas should be extensive and thus proportional to its number of degrees of freedom
 248 (although it is not proportional to the length a). The entropy for the systems of instantons
 249 and anti-instantons $\mathcal{S}_{\text{tunn}}$ is then twice the entropy for the system of pairs, which is given by
 250 the usual sum over probabilities

$$\mathcal{S}_{\text{tunn}} = -2 \sum_{n=0}^{\infty} p_n \ln(p_n). \quad (34)$$

251 In the limit $\bar{N} \gg 1$, we find numerically that the entropy (34) is asymptotically equivalent to

$$\begin{aligned} \mathcal{S}_{\text{tunn}} &\approx \ln(\bar{N}) \\ &= \ln(m\beta) - I_{\text{inst}} + \frac{1}{2} \ln\left(\frac{6}{\pi} I_{\text{inst}}\right), \end{aligned} \quad (35)$$

252 where I_{inst} is the instanton action as given in (16), and the result matches the usual micro-
 253 canonical entropy for \bar{N} microstates. As expected, one can also check that $\mathcal{S}_{\text{tunn}}$ vanishes in the
 254 limit $a \rightarrow \infty$ (where $\bar{N} \rightarrow 0$, even for zero temperature), since tunnelling is then completely
 255 suppressed. This behaviour is in correspondence with an "effective third law of thermodynam-
 256 ics", where $1/a$ plays the role of a temperature. We will come back to this analogy later in this
 257 article.

258 For a finite length a , the entropy is non-zero with a logarithmic divergence in the zero
 259 temperature limit. Such logarithmic divergences in the zero temperature entropy of a quantum
 260 system are not new, such as the massless Casimir effect [34] and it was argued in [35] that
 261 such divergences should be removed.

262 The isothermal compressibility, defined as

$$K \equiv -\frac{1}{a} \frac{\partial a}{\partial p} \equiv \frac{1}{a} \left(\frac{\partial^2 F_{\text{true}}}{\partial a^2} \right)^{-1}, \quad (36)$$

263 is negative for all a , which is usually interpreted as a sign of instability. One may think that
 264 this instability is similar to the one obtained for a Van der Waals fluid experiencing an isother-
 265 mal compression. If one assumes homogeneity of the Van der Waals fluid in a volume V , the
 266 bulk modulus $-V \partial p / \partial V$ is negative in a given range of volumes, which is not physical. What
 267 happens is that the fluid separates into two phases, liquid and vapour, leading to the Maxwell
 268 construction, which corresponds to a constant-pressure plateau. The position of this plateau
 269 is determined by identifying the chemical potentials in each phase. Also, a constant pressure
 270 leads to a vanishing compressibility, and the true free energy is convex, as expected for the

271 Legendre transform of the internal energy. This constant-pressure plateau allows random re-
 272 gions of one vacuum or the other, in a proportion given by the volume, which varies between
 273 values corresponding to the first drop of liquid and the last bubble of vapour.

274 In our case, the system remains homogeneous though: the effective potential does not fea-
 275 ture any plateau, but it has a unique minimum at $\langle \phi \rangle = 0$. An intuitive description is provided
 276 by weakly-interacting spins on a lattice, each with a random direction and a vanishing average
 277 value.⁴ A flat effective potential would be obtained in the limit $ma \rightarrow \infty$, where the tunnelling
 278 rate exponentially vanishes though, in which case one would have to wait an infinite amount
 279 of time for the true vacuum to settle. As mentioned in section 2.1, in our situation the insta-
 280 bility indicated by the negative compressibility would correspond to a spacetime expansion, if
 281 no environment was present to fix the length a .

282 3 Black holes in 1+1 dilaton gravity

283 The study of Hawking radiation including its backreaction on the spacetime geometry is an
 284 extremely difficult problem in 3+1 dimensions. Motivated by dimensional reduction, it is pos-
 285 sible to simplify the problem by studying the 1+1 dimensional case. In particular, we focus
 286 on the classical Callan, Giddings, Harvey and Strominger (CGHS) two-dimensional dilatonic
 287 black hole model [36, 37]. For the semi-classical description of the theory including backre-
 288 action, we consider the standard Polyakov term which represents the leading order quantum
 289 fluctuations in a $1/N$ expansion where N is the number of matter fields. To find analytical
 290 solutions to the semiclassical theory it is necessary to introduce suitable counterterms in the
 291 action. To consider these counterterms, we introduce the one-parameter family of models that
 292 ranges between the Russo, Susskind and Thorlacius (RST) model [38] and the Bose, Parker,
 293 Peleg (BPP) model [39], following the parameterization of the action presented in [40]. We
 294 focus our study on the BPP model since it results in simpler expressions for the metric and the
 295 dilaton.

296 After describing the solutions of the semi-classical theory, this section delves into the im-
 297 plications for the stress-energy tensor and the entropy of two-dimensional black holes.

298 3.1 Introduction to dilaton gravity

299 In two dimensions, the Einstein-Hilbert action is just the Euler characteristic of the manifold
 300 (accordingly, $G_{\mu\nu}$ vanishes identically), and 1+1 dimensional gravity is trivial. Since we want
 301 to capture aspects of the 3+1 dimensional theory within a 1+1 dimensional description, we
 302 use the dilaton field [41, 42] which emerges from the compactification of higher dimensions.
 303 Here, we derive the dilaton from the dimensional reduction of spherically symmetric gravity
 304 in 3+1 dimensions.

305 We consider the 3+1 Einstein-Hilbert action

$$I_{EH}^{(4)} = \frac{1}{16\pi G^{(4)}} \int d^4x \sqrt{-g^{(4)}} R^{(4)}, \quad (37)$$

306 where $^{(4)}$ indicates the spacetime dimension and $G^{(4)}$ is Newton's constant. We consider the
 307 spherically symmetric ansatz

$$ds_{(4)}^2 = g_{ab} dx^a dx^b + \frac{e^{-2\phi(x^a)}}{\lambda^2} (d\theta^2 + \sin^2 \theta d\varphi^2), \quad (38)$$

⁴This is different from the high-temperature limit, where thermal fluctuations dominate over spin interactions and lead to a random spin distribution. The vanishing average spin discussed here happens at zero temperature, and is due to tunnelling instead

308 where the radius r of the 2-sphere has been parametrized via a dilaton field $\phi(x^a)$, $r = \lambda^{-1}e^{-\phi}$.
 309 The parameter λ is dimensionful and is introduced to get a dimensionless dilaton. Using this
 310 ansatz, we can write $R^{(4)}$ in terms of $R \equiv R^{(2)}$ and the four dimensional volume element in
 311 terms of the two-dimensional volume element times the angular terms [43, 44]

$$\begin{aligned} R^{(4)} &= R + 2(\nabla\phi)^2 + 2\lambda^2 e^{2\phi} - 2e^{2\phi} \square e^{-2\phi}, \\ d^4x \sqrt{-g^{(4)}} &= d^2x d\theta d\varphi \sqrt{-g} \frac{e^{-2\phi}}{\lambda^2} \sin^2\theta. \end{aligned} \quad (39)$$

312 Integrating out the angular part, the resulting dilaton action is [43, 44]

$$I_D = \frac{1}{4\pi\lambda^2 G^{(4)}} \int d^2x \sqrt{-g} (e^{-2\phi} (R + 2(\nabla\phi)^2) + 2\lambda^2), \quad (40)$$

313 where we see that λ plays the role of a cosmological constant in the reduced theory. We define
 314 a two dimensional Newton's constant $G^{(2)} = \lambda^2 G^{(4)}$ and work in units where $G^{(4)} = \frac{1}{2\lambda^2}$.

315 To simplify the theory in such a way that it is possible to find an exact analytical solution,
 316 we work with the action⁵

$$I_\phi = \frac{1}{2\pi} \int d^2x \sqrt{-g} e^{-2\phi} (R + 4(\nabla\phi)^2 + 4\lambda^2), \quad (41)$$

317 where we have modified the potential term of the dilation and the coefficient of the kinetic
 318 term as compared with (40). Despite the changes, this dilaton theory still has black holes and
 319 Hawking radiation [36, 37, 46]. We work in conformal gauge,

$$ds^2 = -e^{2\eta} dx^+ dx^-, \quad (42)$$

320 with null coordinates x^\pm . The EoM resulting from the variation of the action with respect to
 321 η and ϕ can be conveniently written in terms of $2(\eta - \phi)$ and $e^{-2\phi}$, namely

$$\partial_+ \partial_- e^{-2\phi} + \lambda^2 e^{2(\eta-\phi)} = 0, \quad (43)$$

$$2e^{-2\phi} \partial_+ \partial_- (\eta - \phi) + \partial_+ \partial_- e^{-2\phi} + \lambda^2 e^{2(\eta-\phi)} = 0. \quad (44)$$

322 Additionally, we derive the following constraints from the variation of the action with respect
 323 to the (\pm, \pm) components of the metric $g_{\mu\nu}$

$$\partial_\pm^2 e^{-2\phi} - 2\partial_\pm (\eta - \phi) \partial_\pm e^{-2\phi} = 0. \quad (45)$$

324 Combining equations (44) and (43) we get the free field equation

$$2\partial_+ \partial_- (\eta - \phi) = 0, \quad (46)$$

325 which has solutions of the form $2(\eta - \phi) = h(x^+) + s(x^-)$. In the Kruskal gauge, the remaining
 326 freedom is fixed by making $h(x^+) = s(x^-) = 0$, i.e. $\eta = \phi$. This model has black hole solutions
 327 which, in the Kruskal gauge, are (see [36, 43] for a detailed discussion)

$$ds^2 = -\frac{dx^+ dx^-}{(M/\lambda - \lambda^2 x^+ x^-)}, \quad (47)$$

$$\eta = \phi = -\frac{1}{2} \ln\left(\frac{M}{\lambda} - \lambda^2 x^+ x^-\right), \quad (48)$$

⁵ I_ϕ can be exactly derived by integrating out the angular part of near-extreme, magnetically charged black holes in four-dimensional dilaton gravity [36, 45].

328 where M is an integration constant that corresponds to the ADM mass of the black hole [36].
 329 This metric has a curvature singularity at $\lambda^2 x^+ x^- = M/\lambda$ and horizons at $\lambda^2 x^+ x^- = 0$, see
 330 figure 3. The surface gravity can be easily computed, and reads $\kappa = \lambda$. Therefore, the black
 331 hole temperature is

$$T = \frac{\lambda}{2\pi}. \quad (49)$$

332 In contrast to the black hole temperature in four dimensions, the two-dimensional black hole
 333 temperature is independent of the mass M . We use these results to evaluate the NEC and the
 334 entropy.

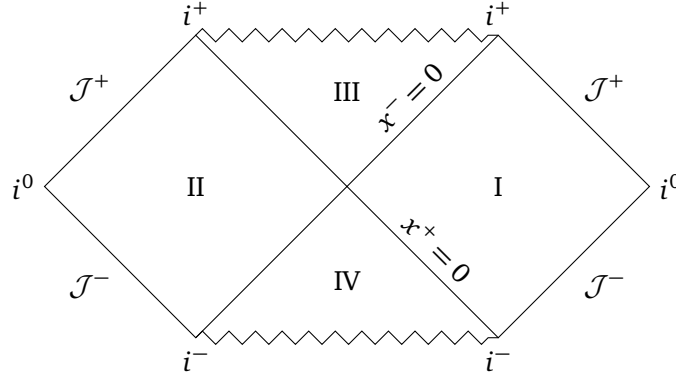


Figure 3: Penrose diagram for a static two-dimensional dilatonic black hole.

335 3.2 Adding quantum matter: static black holes

336 Now we add N massless scalar fields f_i and we have the total action

$$I_0 = I_\phi + I_f = \frac{1}{2\pi} \int d^2x \sqrt{-g} \left[e^{-2\phi} (R + 4(\nabla\phi)^2 + 4\lambda^2) - \frac{1}{2} \sum_{i=1}^N (\nabla f_i)^2 \right]. \quad (50)$$

337 This action corresponds to the CGHS model. We continue the analysis in conformal gauge
 338 (42). In these coordinates, the classical stress-energy tensor for the fields f_i is

$$T_{\pm\pm} = \frac{1}{2} \sum_{i=0}^N (\partial_{\pm} f_i)^2. \quad (51)$$

339 The next step is to quantise the theory. We want to focus on static solutions, $\langle f_i \rangle = 0$, and look
 340 at the one-loop quantum corrections to the stress-energy tensor in different vacuum states. The
 341 quantum corrections of the different fields that we have seen in the CGHS model contribute to
 342 the semiclassical theory. In order to make the analysis feasible, we assume that the number of
 343 matter fields N is very large and calculate the effective action at leading order in an expansion
 344 in $1/N$. In this limit, the quantum fluctuations of the dilaton and the metric can be ignored
 345 and we only have to consider the one-loop correction of the matter fields to the stress-energy
 346 tensor [37, 47, 48]. This one-loop correction to $T_{\mu\nu}$ due to the N massless scalar fields can
 347 be evaluated using the trace anomaly, which relates the expectation value of the stress-energy
 348 tensor and the Ricci scalar [49]

$$\langle T \rangle = \frac{N}{24} R. \quad (52)$$

349 In conformal gauge, the trace anomaly leads to

$$\langle T_{+-} \rangle = -\frac{N}{12} \partial_+ \partial_- \eta. \quad (53)$$

350 In addition, we can use $\langle T_{+-} \rangle$ in (53) together with the conservation of the stress-energy tensor
 351 to determine $\langle T_{\pm\pm} \rangle$

$$\langle T_{\pm\pm} \rangle = -\frac{N}{12} (\partial_{\pm}\eta\partial_{\pm}\eta - \partial_{\pm}^2\eta + t_{\pm}), \quad (54)$$

352 where t_{\pm} is fixed by boundary conditions (vacuum choice). We will analyse two vacuum
 353 choices: the Hartle-Hawking vacuum, which describes thermal equilibrium at infinity and is
 354 given by $t_{\pm} = 0$, and the Boulware vacuum, which describes empty space at infinity and is
 355 given by the boundary conditions $t_{\pm} = -\frac{1}{4(x^{\pm})^2}$.

356 Alternatively, the expectation value of the stress-energy tensor can be obtained by func-
 357 tional differentiation of an effective action, the Polyakov action

$$\langle T_{\mu\nu} \rangle = -\frac{2\pi}{\sqrt{-g}} \frac{\delta I_P}{\delta g^{\mu\nu}}, \quad (55)$$

358 where

$$I_P = -\frac{N}{96\pi} \int d^2x \sqrt{-g(x)} \int d^2y \sqrt{-g(y)} R(x) G(x, y) R(y). \quad (56)$$

359 $G(x, y)$ is the Green's function for the differential operator \square_g . I_P incorporates the backre-
 360 action of the quantum fluctuations of the matter fields on the metric. By writing I_P in the
 361 conformal gauge, we can derive immediately Eqs. (53) and (54) from (55). We will use these
 362 expressions later on in the evaluation of the NEC.

363 It is convenient to convert the non-local Polyakov action into a local one by introducing an
 364 auxiliary scalar field φ constrained to obey the equation $\square_g \varphi = R$ (see for example eq. (5.56)
 365 in [43]). By doing this, the local action is

$$I_P = -\frac{N}{96\pi} \int d^2x \sqrt{-g(x)} (\varphi \square_g \varphi + 2\varphi R). \quad (57)$$

366 In conformal gauge, the equation of motion for φ has the following solution

$$\varphi(x^{\pm}) = -2\eta(x^{\pm}) + 2(\varphi_+(x^+) + \varphi_-(x^-)), \quad (58)$$

367 where $\varphi_+(x^+)$ and $\varphi_-(x^-)$ are solutions of

$$-(\partial_{\pm}\varphi_{\pm})^2 + \partial_{\pm}^2\varphi_{\pm} = t_{\pm}(x^{\pm}). \quad (59)$$

368 We are also interested in the entropy of the system. As we showed in (47), this theory
 369 has black hole solutions. Therefore, the total entropy of the system consists of two terms: the
 370 geometric black hole entropy, which is the 1 + 1 dimensional equivalent of the Bekenstein-
 371 Hawking entropy, and the von Neuman entropy, associated to the quantum fields outside the
 372 horizon, usually called fine-grained entropy [37, 50, 51]. For general diffeomorphism invari-
 373 ant theories, it is possible to evaluate both of these entropies using the method developed in
 374 ref. [52] and particularised to the context of two-dimensional gravity in Refs. [50, 51, 53]. In
 375 this way, both entropies can be evaluated in a geometrical way by calculating the derivatives
 376 of the Lagrangian associated with the different contributions to the action with respect to the
 377 curvature

$$\mathcal{S}_{\phi} = \frac{4\pi}{\sqrt{-g}} \frac{\partial \mathcal{L}_{\phi}}{\partial R} \Big|_H = 2e^{-2\phi} \Big|_H \quad (60)$$

$$\mathcal{S}_P = \frac{4\pi}{\sqrt{-g}} \frac{\partial \mathcal{L}_P}{\partial R} \Big|_H = -\frac{N}{12} \varphi \Big|_H, \quad (61)$$

378 where $|_H$ means that these quantities should be evaluated at the horizon. It can be shown
 379 that \mathcal{S}_ϕ and \mathcal{S}_p are equivalent to the black hole and the fine-grained entropy respectively
 380 [37, 51, 54]. Equivalently, the entropy can be evaluated using the Euclidean path integral
 381 approach, as done in ref. [55] for the RST model.

382 In what follows, we proceed to evaluate the NEC and the entropy. We start with the simpler
 383 case without backreaction, and then we study how backreaction modifies the results.

384 3.3 Without backreaction, the CGHS model

385 For the case without backreaction, the background spacetime is described by (50), i.e. the
 386 CGHS model. Since we are interested in static black holes, we focus on the case where $\langle f \rangle = 0$.
 387 As we have seen, under these conditions, the solution is an eternal black hole of mass M .

388 3.3.1 Null energy condition

389 The null energy condition

$$\langle T_{\mu\nu} \rangle \ell^\mu \ell^\nu \geq 0, \quad (62)$$

390 gives two equations that, in the conformal gauge, are proportional to the diagonal components
 391 of the stress-energy tensor $\langle T_{\pm\pm} \rangle$. In what follows, we will focus on the exterior region, so
 392 we assume $x^+ > 0$ and $x^- < 0$. For the Hartle-Hawking vacuum ($t_\pm = 0$), using the dilatonic
 393 metric (48) in eq. (54), we find⁶

$$NEC_H^\pm = (\lambda x^\pm)^2 \langle H | T_{\pm\pm} | H \rangle = \frac{N \lambda^2}{48} (\lambda x^\pm)^2 (\lambda x^\mp)^2 e^{4\eta} > 0, \quad (63)$$

394 while for the Boulware vacuum we obtain

$$NEC_B^\pm = (\lambda x^\pm)^2 \langle B | T_{\pm\pm} | B \rangle = -\frac{N \lambda^2}{48} (1 - (\lambda x^\pm)^2 (\lambda x^\mp)^2 e^{4\eta}) < 0. \quad (64)$$

395 We can easily check that the difference between the Hartle-Hawking and Boulware stress
 396 energy tensors is just a thermal distribution of massless particles at the Hawking temperature⁷

$$NEC_H^\pm - NEC_B^\pm = N \frac{\lambda^2}{48} = N \frac{\pi^2}{12} T^2, \quad (65)$$

397 where $T = \lambda/2\pi$ is the black hole temperature as given in eq. (49). The extra N factor
 398 appears because we are considering N conformal fields. For convenience, we can write the
 399 stress-energy tensor in the Hartle-Hawking vacuum as

$$NEC_H^\pm = \frac{N \lambda^2}{48} - \frac{N \lambda^2}{48} (1 - (\lambda x^\pm)^2 (\lambda x^\mp)^2 e^{4\eta}) > 0. \quad (66)$$

400 In this expression, we see that there is a negative contribution coming from pure vacuum
 401 effects plus a positive contribution coming from thermal effects. As a final note, we point out
 402 that the quantity $(1 - (\lambda x^\pm)^2 (\lambda x^\mp)^2 e^{4\eta})$ vanishes as $x^\pm \rightarrow \pm\infty$ and tends to 1 as $x^\pm \rightarrow 0$.
 403 It means that $(\lambda x^+)^2 \langle H | T_{++} | H \rangle \rightarrow N \lambda^2/48$ asymptotically (constant thermal flux), and goes
 404 to zero at the horizon (thermal bath in thermal equilibrium with the black hole, so the fluxes

⁶The condition $\langle T_{\mu\nu} \rangle \ell^\mu \ell^\nu \geq 0$ is defined up to a positive overall factor. In this case, we find it useful to compute $(\lambda x^\pm)^2 \langle T_{\pm\pm} \rangle$ instead of $\langle T_{\pm\pm} \rangle$, since it is the quantity related to an asymptotic observer at infinity. This quantity comes directly from the transformation law for tensors $T_{\nu\nu} = (dx^+/d\nu)^2 T_{++}$ (and similarly for the other components).

⁷See ref. [56] for a similar analysis in a Schwarzschild background.

405 cancel). We can remove the contribution from the thermal bath to compute the NEC vacuum
 406 contribution of the black hole

$$NEC_{\text{BH}} = (\lambda x^\pm)^2 \langle H | T_{\pm\pm} | H \rangle - \left(\frac{N \lambda^2}{48} \right) = -\frac{N \lambda^2}{48} (1 - (\lambda x^\pm)^2 (\lambda x^\mp)^2 e^{4\eta}) < 0, \quad (67)$$

407 which results in a negative contribution to the NEC due to vacuum effects. On the horizon

$$NEC_{\text{BH}} = -\left(\frac{N \pi^2 T^2}{12} \right). \quad (68)$$

In figure 4 we summarise the results for the NEC.

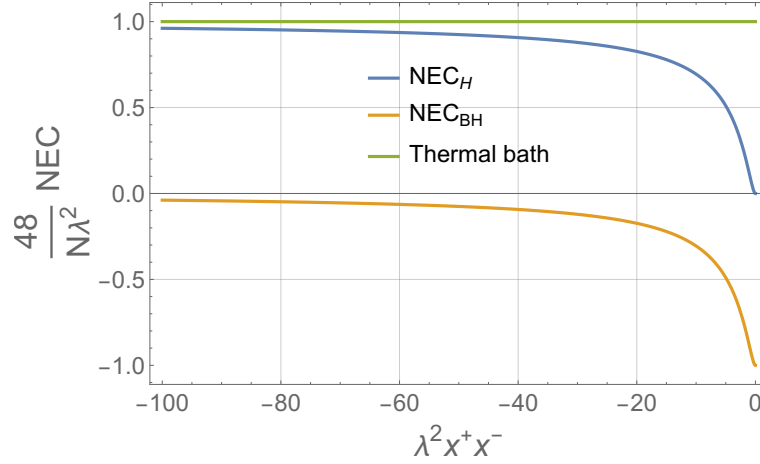


Figure 4: We plot the (normalized) energy condition $\frac{48}{N\lambda^2}$ (NEC) as a function of $\lambda^2 x^+ x^-$ for the BPP and classical models. The green curve corresponds to the thermal bath eq. (65), the orange curve corresponds to the contribution from vacuum effects eq. (64), and the total NEC eq. (66) is represented in blue. The black hole mass is $M/\lambda = 2$.

408

409 3.3.2 Entropy and thermodynamics

410 Inserting the dilaton solution (48) into (60), the black hole entropy is

$$\mathcal{S}_{\text{BH}} = \mathcal{S}_\phi = \frac{2M}{\lambda} = \frac{M}{\pi T}. \quad (69)$$

411 From the dimensional reduction (38) relating the radius and the dilaton, we can interpret this
 412 term as 1/4 of the horizon area of the classical 3 + 1-dimensional black hole. Remember that
 413 in the dimensional reduction (38), $r = \lambda^{-1} e^{-\phi}$ and $\mathcal{S}_\phi = 2e^{-2\phi_H} = \frac{2\lambda^2}{\pi} \frac{4\pi r_H^2}{4}$ (see eq. (60)).

414 To evaluate the entropy associated with the N massless fields surrounding the black hole
 415 we use (61). Although we are not considering backreaction in this subsection, we can still
 416 evaluate \mathcal{S}_p using the classical solution (48) to obtain the fine-grained entropy of the matter
 417 fields. In the Hartle-Hawking vacuum ($t_\pm(x^\pm) = 0$), the auxiliary field φ is [see Eqs. (58) and
 418 (59)]

$$\varphi = -2\eta - \ln(-\lambda^2 x^+ x^-) + \text{const}. \quad (70)$$

419 which means that there is a logarithmic divergence when evaluated at the horizon. However,
 420 its contribution to the entropy can be easily understood in terms of the entropy of a thermal
 421 bath. Indeed, if we rewrite the log term in light-cone coordinates

$$x^+ = \lambda^{-1} e^{\lambda\sigma^+}, \quad \text{and} \quad x^- = -\lambda^{-1} e^{-\lambda\sigma^-}, \quad (71)$$

422 we obtain

$$-\frac{N}{12} \ln(-\lambda^2 x^+ x^-) \Big|_H = \frac{N}{12} \lambda(\sigma^- - \sigma^+) \Big|_H = \frac{N}{12} \lambda(2L) = \frac{N\pi}{6} T(2L) = \mathcal{S}_{thermal} \quad (72)$$

423 which is exactly the entropy of a thermal bath in an one dimensional box of length $2L = (\sigma^- - \sigma^+) \Big|_H$,
 424 as seen by an asymptotic observer. Since the length is infinite, $(\sigma^- - \sigma^+ = -2x \rightarrow \infty$ at the
 425 horizon), the entropy diverges. This result allows us to rewrite the entropy of the Polyakov
 426 term as

$$\mathcal{S}_p = \mathcal{S}_{quantum} + \mathcal{S}_{thermal}, \quad (73)$$

427 where

$$\mathcal{S}_{quantum} = \frac{N}{6} \eta \Big|_H = -\frac{N}{12} \ln\left(\frac{M}{\lambda}\right). \quad (74)$$

428 The Polyakov entropy matches the fine-grained entropy given in eq. (93) of [37] for an eter-
 429 nal black hole. This is easily done by identifying our $\mathcal{S}_{thermal}$ with the $\frac{N}{12} \ln(-x_{\max}^+ x_{\max}^- / \delta^2)$
 430 term. In ref. [37], the x_{\max}^\pm are infrared cut-offs for the right and left moving modes and
 431 δ is a short distance cut-off introduced to regularize the logarithmic ultraviolet divergence
 432 arising from the entanglement of the short-wavelength field fluctuations at the edge of the
 433 horizon [54].

434 In what follows, we will subtract the thermal contribution to the entropy, since we want
 435 to focus on vacuum effects. Now, the total entropy of the system is (excluding $\mathcal{S}_{thermal}$)

$$\mathcal{S}_{tot} = \mathcal{S}_{BH} + \mathcal{S}_{quantum} = \frac{2M}{\lambda} - \frac{N}{12} \ln\left(\frac{M}{\lambda}\right), \quad (75)$$

436 where we have used that, in the Kruskal gauge, $\phi = \eta$ is given by eq. (48).

437 3.4 With backreaction, the BPP model

438 As we discussed, the backreaction on the metric of the quantum fluctuations of the matter
 439 field can be considered by adding I_p to the action I_ϕ . However, the EoM from $I_\phi + I_p$ can not
 440 be solved analytically. To address this problem, we can add the following extra term to the
 441 action [40]

$$\begin{aligned} I_{extra} &= \frac{N}{24\pi} \int d^2x \sqrt{-g} [(1-2b)(\nabla\phi)^2 + (b-1)\phi R] \\ &= \frac{N}{24\pi} \int d^2x (-2(1-2b)\partial_+\phi\partial_-\phi + 4(b-1)\phi\partial_+\partial_-\eta). \end{aligned} \quad (76)$$

442 This results in a family of models characterized by the parameter b . I_{extra} being local modifies
 443 the local dynamics but not the global properties. For $b = 1/2$ we recover the RST model [38]
 444 and for $b = 0$ we recover the BPP model [39]. By introducing the Liouville fields [40]

$$\Omega = \sqrt{\frac{N}{12}} b\phi + \sqrt{\frac{12}{N}} e^{-2\phi}, \quad (77)$$

$$\chi = \sqrt{\frac{N}{12}} \eta + \sqrt{\frac{N}{12}} (b-1)\phi + \sqrt{\frac{12}{N}} e^{-2\phi}, \quad (78)$$

445 we can rewrite our family of models as a Liouville theory that can be solved analytically. The
 446 EoM for the action $I_\phi + I_p + I_{extra}$ in terms of the Liouville variables are

$$\partial_+\partial_-\chi = -\lambda^2 \sqrt{\frac{12}{N}} e^{\sqrt{\frac{48}{N}}(\chi-\Omega)}, \quad (79)$$

$$\partial_+\partial_-\Omega = -\lambda^2 \sqrt{\frac{12}{N}} e^{\sqrt{\frac{48}{N}}(\chi-\Omega)}, \quad (80)$$

447 which implies

$$\partial_+ \partial_- (\chi - \Omega) = 0. \quad (81)$$

448 The constraint equations become

$$-\partial_\pm \chi \partial_\pm \chi + \sqrt{\frac{N}{12}} \partial_\pm^2 \chi + \partial_\pm \Omega \partial_\pm \Omega - \frac{N}{12} t_\pm = 0. \quad (82)$$

449 In the Kruskal gauge $\Omega = \chi$ and for the Hartle-Hawking vacuum ($t_\pm = 0$) we have the solution

$$\sqrt{\frac{N}{12}} \Omega = \frac{M}{\lambda} - \lambda^2 x^+ x^-. \quad (83)$$

450 From now on, we focus on the model $b = 0$, i.e. the BPP model, since it results in a simpler
451 solution. Taking $b = 0$ and (83) into the Liouville variables (77) and (78), it is immediate to
452 find

$$\phi = \eta = -\frac{1}{2} \ln \left(\frac{M}{\lambda} - \lambda^2 x^+ x^- \right). \quad (84)$$

453 These solutions are the same as the classical solutions (48), which indicates that the metric
454 and the dilaton do not have quantum corrections in the BPP model.

455 3.4.1 Null energy condition

456 The results for the NEC in section 3.3.1 don't change when we consider the BPP model in the
457 Hartle-Hawking vacuum since the metric is not affected by the quantum corrections. Figure 4
458 summarizes the results for the NEC in the BPP model and the classical results.

459 3.4.2 Entropy and thermodynamics

460 The evaluation of the entropy follows the discussion in section 3.3.2. Since we included the
461 $I_{bpp} = I_{extra}(b = 0)$ term in the action, we have an additional contribution to the entropy

$$\mathcal{S}_{bpp} = \frac{4\pi}{\sqrt{-g}} \frac{\partial \mathcal{L}_{bpp}}{\partial R} \Big|_H = -\frac{N}{6} \phi \Big|_H = \frac{N}{12} \ln \left(\frac{M}{\lambda} \right). \quad (85)$$

462 The total entropy of the semi-classical system is (as before, we omit the $\mathcal{S}_{thermal}$ contribution
463 of \mathcal{S}_p)

$$\mathcal{S}_{tot} = \mathcal{S}_\phi + \mathcal{S}_{bpp} + \mathcal{S}_{quantum} = 2e^{-2\phi} \Big|_H = \frac{2M}{\lambda}, \quad (86)$$

464 where we have used that, in the Kruskal gauge $\phi = \eta$, and the dilaton is given by (48). Note
465 that \mathcal{S}_{bpp} cancels with $\mathcal{S}_{quantum}$. We find that \mathcal{S}_{tot} is equal to the \mathcal{S}_{BH} for the case without
466 backreaction (69). It means that the total entropy of the semi-classical system is exactly the
467 entropy of a dilatonic black hole of mass M at a temperature $\lambda/2\pi$. This is not surprising since
468 the solution to the semi-classical equations in the Hartle-Hawking vacuum state is precisely a
469 black hole of mass M at a temperature $\lambda/2\pi$. However, we can still split the total entropy into
470 two parts: the entropy of the black hole, and the entropy of the matter sector

$$\mathcal{S}_{BH} = \mathcal{S}_\phi + \mathcal{S}_{bpp} = \frac{2M}{\lambda} + \frac{N}{12} \ln \left(\frac{M}{\lambda} \right), \quad (87)$$

$$\mathcal{S}_{quantum} = -\frac{N}{12} \ln \frac{M}{\lambda}. \quad (88)$$

471 The matter entropy $\mathcal{S}_{quantum}$ is negative just because we removed the log divergent contribu-
472 tion coming from the thermal bath. Let us note that \mathcal{S}_{BH} has a quantum correction as compared
473 to the black hole entropy without backreaction (69) coming from \mathcal{S}_{bpp} .

474 We finally comment on a related quantity, which is the black hole heat capacitance for the
475 complete system (see Eqs. (86) and (72))

$$C_{tot} = T \frac{\partial(\mathcal{S}_{tot} + \mathcal{S}_{thermal})}{\partial T} = \frac{\pi NTL}{3} - \frac{M}{\pi T}, \quad (89)$$

476 and which is consistently positive, due to the dominant contribution of the thermal bath. Thus
477 the full system is thermodynamically stable.

478 4 Comparison

479 In sections 2 and 3 we discussed the thermodynamics of finite volume effects in QFT and dila-
480 tonic black holes respectively. These effects seem at first glance unrelated. However, in both
481 systems we have NEC violation and finite quantum entropy. But the analogy runs even deeper;
482 we observe that the effect of the temperature T in black holes is similar to the effect of the
483 inverse length scale $1/a$ in tunneling. To see this, we compare two physical quantities, which
484 are the NEC and the rate of change in entropy, when the environment is modified.

485

486 *NEC violation.*

487 For tunneling, the NEC was computed in section 2.3. We will compare in the regime where
488 $ma \lesssim 1$, where the NEC becomes

$$NEC_{tun} \approx -\frac{\pi}{3a^2}. \quad (90)$$

489 It is interesting to note that in this regime the Casimir effect is dominant over the tunneling
490 effects. The result on the black hole horizon for any ratio T/M in the BPP model is computed
491 in section 3

$$NEC_{BH} = -\frac{N\pi^2 T^2}{12}. \quad (91)$$

492 We notice the clear equivalence of the dominant terms in the regime of interest: NEC violation
493 is proportional to $1/a^2$ and T^2 for the tunneling and the black hole respectively. Physically,
494 this is partly a manifestation of the effect that the NEC violation is due to finite volume effects
495 in one case and the non-zero temperature of the black hole in the other.

496

497 *Entropy*

498 For the tunneling case we found (Sec. 2.4)

$$\mathcal{S}_{tun} = \ln(m\beta) - \frac{2ma}{3} + \frac{1}{2} \ln\left(\frac{4ma}{\pi}\right). \quad (92)$$

499 The black hole entropy is (Sec. 3.4.2)

$$\mathcal{S}_{BH} + \mathcal{S}_{thermal} = \frac{N\pi}{6} T(2L) + \frac{M}{\pi T} + \frac{N}{12} \ln\left(\frac{M}{2\pi T}\right). \quad (93)$$

500 We note that both entropies have a term that diverges in the limit of zero temperature for
501 the tunneling and the limit of infinite volume for the black hole. These terms are $\ln(m\beta)$ for
502 tunneling and $\frac{N\pi}{6} T(2L)$ for the black hole. We will remove these terms as we want to compare
503 the quantum entropies of the two systems without infinite contributions. Then the entropy in
504 both cases can be negative.

505 Instead of comparing the entropies as they are, we will focus on the rate of change of the
506 entropy in terms of the relevant parameter w for each system

$$R \equiv w \frac{\partial \mathcal{S}}{\partial w}. \quad (94)$$

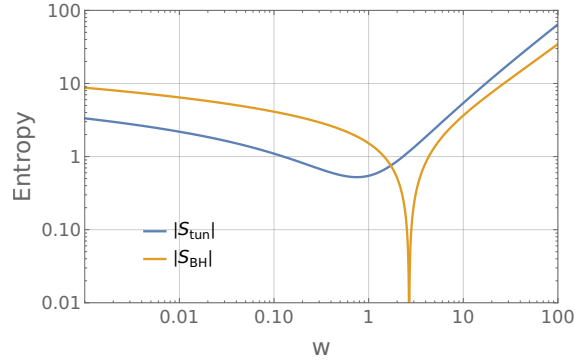


Figure 5: Tunneling (92) and black hole (93) entropies as a function of $w = ma$ and $w = \frac{M}{T}$, respectively. We have removed the $\ln(m\beta)$ divergence and set $N = 12$.

507 So we consider the rate of change in entropy when the length a varies

$$R_{\text{tun}} \equiv a \frac{\partial \mathcal{S}_{\text{tun}}}{\partial a} = \frac{1}{2} - \frac{2m}{3} a . \quad (95)$$

508 For the black hole case, the rate of change is in terms of the temperature

$$R_{\text{BH}} \equiv T \frac{\partial \mathcal{S}_{\text{BH}}}{\partial T} = -\frac{N}{12} - \frac{M}{\pi T} . \quad (96)$$

509 As for NEC violation, we observe that there is a clear equivalence of the rates of change in
 510 entropy when one maps a to $1/T$. This is not an effect that can be explained by simple di-
 511 mensional analysis: the quantities ma and T/M are dimensionless and thus any combination
 512 could appear in these expressions.

513 Fig. 5 shows the absolute value of \mathcal{S}_{tun} and \mathcal{S}_{BH} as a function of ma and M/T , respectively.
 514 Without the term $\ln(m\beta)$, \mathcal{S}_{tun} is always negative because of the dominant contribution of the
 515 negative linear term. For \mathcal{S}_{BH} , the positive linear term becomes dominant when M/T exceeds
 516 $\frac{N\pi}{12} W_0(\frac{24}{N})$. The divergence observed in the logarithmic plot indicates a change in the sign of
 517 \mathcal{S}_{BH} at higher temperatures, where the logarithmic term takes over. Although these quantities
 518 can be negative, the total entropy remains positive due to the contributions of $\ln(m\beta)$ and
 519 S_{thermal} .

520 We should briefly comment on a relevant comparison between the Casimir effect and black
 521 hole thermodynamics in refs. [57, 58]. There, the authors used isothermal compressibility
 522 instead of the rate of change of the entropy but also found an analogy.

523 5 Conclusions

524 Motivated by the description of Hawking radiation in terms of NEC violation, we mapped
 525 a few aspects of black hole thermodynamics with finite volume effects in QFT arising from
 526 tunnelling in a confined space. Both descriptions are done in $1 + 1$ dimensions, and feature
 527 similar behaviours in terms of energy and entropy, when one identifies the inverse of the BH
 528 temperature with the finite size of the confining space for a scalar field. The origin of the
 529 mapping is the presence of boundaries in both systems, either in the form of a horizon for the
 530 BH, or in the form of periodic boundary conditions in QFT.

531 We focused the comparison on the regime $ma \propto M/T \lesssim 1$, and not on the regime
 532 $ma \propto M/T \gg 1$. In the latter case, the non-trivial effects vanish exponentially with a for
 533 tunnelling, whereas for the black hole they vanish as a power law with T . In this example, the

534 mapping we discussed does not hold and a more thorough discussion is necessary to include
535 all the regimes in this study, which is left for a future work.

536 One possibility is the approach described in [59], where a massless scalar field on a D -
537 sphere is considered, and a non-minimal coupling to curvature is introduced, which provides
538 an effective mass. The latter depends on the curvature, such that the action of the instanton is
539 not proportional to the volume, and therefore tunnelling is not suppressed exponentially with
540 the volume. In particular, for $D = 3$ NEC violation varies as $1/a$ for all values of a , and such a
541 power law dependence is more likely to match the black hole description. This approach does
542 not modify the picture presented here, but further studies involving $D \geq 2$ space dimensions
543 are necessary.

544 An essential point in our study is the presence of an environment which is necessary to
545 justify the static regimes we study. For tunnelling, this environment fixes the spatial period,
546 whereas for the black hole it plays the role of a heat source and fixes the temperature. Re-
547 moving this environment could also be an avenue to explore, in which case the equilibrium
548 assumption is no longer valid; since the black hole evaporates and the confining space for the
549 scalar field is modified by energetics of NEC violation.

550 Another interesting connection point that was not discussed in this work, is that Hawking
551 radiation can be studied as tunneling of particles through the black hole horizon [60]. Then
552 both systems can be viewed as tunneling, one on a flat background with a finite volume and one
553 on a curved background with an infinite volume. This connection could be explored further
554 in future work, especially in the $3 + 1$ dimensional case.

555 Given the above analogies, we hope to find a more formal description for this mapping in
556 light of the AdS/CFT correspondence, although both systems here have the same dimension-
557 ality. Hopefully such a mapping could be extended to $3+1$ dimensions, and might be relevant
558 to either astrophysics or analogue condensed matter systems.

559 Acknowledgements

560 The authors would like to thank Dionysios Anninos, Jose Navarro-Salas, and Andrew Svesko
561 for useful discussions.

562 **Funding information** The Science and Technology Facilities Council supports the work of
563 JA and DB (grant No. STFC-ST/X000753/1), the Engineering and Physical Sciences Research
564 Council supports the work of JA (grant No. EP/V002821/1) and the Leverhulme Trust sup-
565 ports the work of JA and SP (grant No. RPG-2021-299). DPS is supported by the EPSRC
566 studentship grant EP/W524475/1. For the purpose of Open Access, the authors have applied
567 a CC BY public copyright licence to any Author Accepted Manuscript version arising from this
568 submission.

569 A Casimir effect for static saddle points

570 This appendix is based on the book [9], and we consider periodic boundary conditions in
571 space. We first show the derivation for vanishing temperature (limit $\beta \rightarrow \infty$), for which
572 the ground state energy contains an ultraviolet divergence. We then show how to include
573 finite-temperature effects, which do not introduce new divergences.

574 Evaluating the individual connected graph generating functional $W[\phi_i]$ (10) at the static

575 saddle points $\phi_s = \pm 1$ for vanishing source $j = 0$ yields

$$W[\phi_s] \equiv W_{\text{stat}}(a, \beta) = \frac{1}{2} \sum_{n \in \mathbb{Z}} \sum_{l \in \mathbb{Z}} \ln \left(\frac{\nu_l^2 + \omega_n^2}{\nu_l^2} \right), \quad (\text{A.1})$$

576 where $\omega_n = \sqrt{m^2 + k_n^2}$, and

$$\nu_l = \frac{2\pi l}{\beta}, \quad k_n = \frac{2\pi n}{a}. \quad (\text{A.2})$$

577 The origin of energies is chosen in such a way as to recover the usual sum of ground state
578 energies of harmonic oscillators, at zero temperature.

579 A.1 Zero temperature

580 In the limit of zero temperature the summation over Matsubara modes becomes an integral

$$\lim_{\beta \rightarrow \infty} \{W[\phi_s]\} = \frac{\beta}{2} \sum_{n \in \mathbb{Z}} \int_{-\infty}^{\infty} \frac{d\nu}{2\pi} \ln \left(\frac{\nu^2 + \omega_n^2}{\nu^2} \right) = \frac{\beta}{2} \sum_{n \in \mathbb{Z}} \omega_n. \quad (\text{A.3})$$

581 Using the Abel-Plana formula

$$\sum_{n \in \mathbb{N}} F(n) \equiv -\frac{1}{2} F(0) + \int_0^{\infty} F(t) dt + i \int_0^{\infty} \frac{dt}{e^{2\pi t} - 1} [F(it) - F(-it)], \quad (\text{A.4})$$

582 the sum over the frequencies can be expressed as

$$\sum_{n \in \mathbb{Z}} \omega(n) = 2a\Lambda^2 + 2i \int_0^{\infty} \frac{dt}{e^{2\pi t} - 1} [\omega(it) - \omega(-it)], \quad (\text{A.5})$$

583 where the ultraviolet divergence is

$$\Lambda^2 \equiv \frac{m^2}{2\pi} \int_0^{\infty} \sqrt{t^2 + 1} dt. \quad (\text{A.6})$$

584 By considering the principle branch $z \in]-\infty, 0]$ of $\ln(z)$, we have

$$\omega(it) - \omega(-it) = \frac{4\pi i}{a} \sqrt{t^2 - \mu^2} \theta(t - \mu), \quad (\text{A.7})$$

585 where $\mu \equiv ma/2\pi$. The individual connected graph generating functional for static saddle
586 points therefore reads, in the limit of zero temperature,

$$\lim_{\beta \rightarrow \infty} \{W[\phi_s]\} = a\beta\Lambda^2 - \beta \frac{4\pi}{a} \int_{\mu}^{\infty} \frac{dt}{e^{2\pi t} - 1} \sqrt{t^2 - \mu^2} \quad (\text{A.8})$$

$$= \beta a\Lambda^2 - \beta \frac{m^2 a}{\pi} \int_1^{\infty} \frac{du}{e^{mau} - 1} \sqrt{u^2 - 1}. \quad (\text{A.9})$$

587 A.2 Finite-temperature corrections

588 In order to calculate thermal corrections to the individual connected graph generating func-
589 tional for static saddle points, we employ the zeta-function regularisation and write the ex-
590 pression (11) as

$$W_{\text{stat}}(a, \beta, s) = -\frac{1}{2} \frac{\partial}{\partial s} \left(\sum_{l \in \mathbb{Z}} \sum_{n \in \mathbb{Z}} (\beta a)^{-s} (\nu_l^2 + \omega_n^2)^{-s} \right), \quad (\text{A.10})$$

591 where the ultraviolet divergence is turned into a divergence in the limit $s \rightarrow 0$. The above can
592 be written in terms of a parametric integral

$$W_{\text{stat}}(a, \beta, s) = -\frac{1}{2} \frac{\partial}{\partial s} \left(\int_0^\infty \frac{dt}{t} \frac{t^s}{\Gamma(s)} \sum_{l \in \mathbb{Z}} \sum_{n \in \mathbb{Z}} e^{-t\beta a (v_l^2 + \omega_n^2)} \right). \quad (\text{A.11})$$

593 From the Poisson summation formula, one can derive the following identity

$$\sum_{l \in \mathbb{Z}} e^{-z l^2} = \sqrt{\frac{\pi}{z}} \sum_{l \in \mathbb{Z}} e^{-\pi^2 l^2 / z}, \quad (\text{A.12})$$

594 which, when applied to the Matsubara sum in eq. (A.11) with $z = \beta a t (2\pi T)^2$, leads to

$$W_{\text{stat}}(a, \beta, s) = -\frac{\beta}{2} \frac{\partial}{\partial s} \left(\sum_{l \in \mathbb{Z}} \int_0^\infty \frac{dt}{t} \frac{t^s}{\Gamma(s) \sqrt{4\pi\beta a t}} \sum_{n \in \mathbb{Z}} e^{-\frac{l^2 \beta^2}{4\beta a t} - \beta a t \omega_n^2} \right). \quad (\text{A.13})$$

595 The ultraviolet divergence is contained within the temperature-independent integral for $l = 0$.
596 We thus make the following decomposition of eq. (A.13)

$$W_{\text{stat}}(a, \beta, s) = \lim_{\beta \rightarrow \infty} \{W_{\text{stat}}(a, \beta, s)\} + W_{\text{stat}}^T(a, \beta), \quad (\text{A.14})$$

597 where the temperature independent part is calculated in the previous section, and the temperature-
598 dependent part is given by

$$W_{\text{stat}}^T(a, \beta) \equiv -\frac{\beta}{\sqrt{4\pi\beta a}} \sum_{l \in \mathbb{N}} \int_0^\infty \frac{dt}{t^{3/2}} \sum_{n \in \mathbb{Z}} e^{-\frac{l^2 \beta^2}{4\beta a t} - \beta a t \omega_n^2}. \quad (\text{A.15})$$

599 Note that the regulator has been removed from eq. (A.15) using

$$\lim_{s \rightarrow 0} \left[\frac{\partial}{\partial s} \frac{f(s)}{\Gamma(s)} \right] = f(0). \quad (\text{A.16})$$

600 The integral and summation over l in eq. (A.15) can be then evaluated, leading to

$$W_{\text{stat}}^T(a, \beta) = \sum_{n \in \mathbb{Z}} \ln(1 - e^{-\beta \omega_n}). \quad (\text{A.17})$$

601 References

- 602 [1] S. W. Hawking, *Black hole explosions*, Nature **248**, 30 (1974), doi:[10.1038/248030a0](https://doi.org/10.1038/248030a0).
- 603 [2] E. Curiel, *A Primer on Energy Conditions*, Einstein Stud. **13**, 43 (2017), doi:[10.1007/978-1-4939-3210-8_3](https://doi.org/10.1007/978-1-4939-3210-8_3), [1405.0403](https://arxiv.org/abs/1405.0403).
- 604 [3] E.-A. Kontou and K. Sanders, *Energy conditions in general relativity and quantum field theory*, Class. Quant. Grav. **37**(19), 193001 (2020), doi:[10.1088/1361-6382/ab8fcf](https://doi.org/10.1088/1361-6382/ab8fcf), [2003.01815](https://arxiv.org/abs/2003.01815).
- 605 [4] C. Barcelo and M. Visser, *Scalar fields, energy conditions, and traversable wormholes*, Class. Quant. Grav. **17**, 3843 (2000), doi:[10.1088/0264-9381/17/18/318](https://doi.org/10.1088/0264-9381/17/18/318), [gr-qc/0003025](https://arxiv.org/abs/gr-qc/0003025).
- 606 [5] J. R. Fliss, B. Freivogel, E.-A. Kontou and D. P. Santos, *Non-minimal coupling, negative null energy, and effective field theory* (2023), [2309.10848](https://arxiv.org/abs/2309.10848).
- 607
608
609
610
611

- 612 [6] R. Penrose, *Gravitational collapse and space-time singularities*, Phys. Rev. Lett. **14**, 57
613 (1965), doi:[10.1103/PhysRevLett.14.57](https://doi.org/10.1103/PhysRevLett.14.57).
- 614 [7] S. W. Hawking, *Black holes in general relativity*, Commun. Math. Phys. **25**, 152 (1972),
615 doi:[10.1007/BF01877517](https://doi.org/10.1007/BF01877517).
- 616 [8] H. Epstein, V. Glaser and A. Jaffe, *Nonpositivity of energy density in Quantized field theo-*
617 *ries*, Nuovo Cim. **36**, 1016 (1965), doi:[10.1007/BF02749799](https://doi.org/10.1007/BF02749799).
- 618 [9] M. Bordag, G. L. Klimchitskaya, U. Mohideen and V. M. Mostepanenko, *Advances in the*
619 *Casimir Effect*, doi:[10.1093/acprof:oso/9780199238743.001.0001](https://doi.org/10.1093/acprof:oso/9780199238743.001.0001) (2009).
- 620 [10] J. Alexandre and J. Polonyi, *Symmetry restoration, tunneling, and the null energy con-*
621 *dition*, Phys. Rev. D **106**(6), 065008 (2022), doi:[10.1103/PhysRevD.106.065008](https://doi.org/10.1103/PhysRevD.106.065008),
622 [2205.00768](https://doi.org/10.1093/acprof:oso/9780199238743.001.0001).
- 623 [11] J. Alexandre and D. Backhouse, *Null energy condition violation: Tunneling versus the*
624 *Casimir effect*, Phys. Rev. D **107**(8), 085022 (2023), doi:[10.1103/PhysRevD.107.085022](https://doi.org/10.1103/PhysRevD.107.085022),
625 [2301.02455](https://doi.org/10.1093/acprof:oso/9780199238743.001.0001).
- 626 [12] J. Alexandre and S. Pla, *Cosmic bounce and phantom-like equation of state from tunnelling*,
627 JHEP **05**, 145 (2023), doi:[10.1007/JHEP05\(2023\)145](https://doi.org/10.1007/JHEP05(2023)145), [2301.08652](https://doi.org/10.1093/acprof:oso/9780199238743.001.0001).
- 628 [13] J. Alexandre, K. Clough and S. Pla, *Tunneling-induced cosmic bounce in the presence of*
629 *anisotropies*, Phys. Rev. D **108**(10), 103515 (2023), doi:[10.1103/PhysRevD.108.103515](https://doi.org/10.1103/PhysRevD.108.103515),
630 [2308.00765](https://doi.org/10.1093/acprof:oso/9780199238743.001.0001).
- 631 [14] W.-Y. Ai, J. Alexandre, M. Carosi, B. Garbrecht and S. Pla, *Double-well instantons in finite*
632 *volume*, JHEP **05**, 099 (2024), doi:[10.1007/JHEP05\(2024\)099](https://doi.org/10.1007/JHEP05(2024)099), [2402.09863](https://doi.org/10.1093/acprof:oso/9780199238743.001.0001).
- 633 [15] X.-Y. Hu, M. Kleban and C. Yu, *Electric field decay without pair produc-*
634 *tion: lattice, bosonization and novel worldline instantons*, JHEP **03**, 197 (2022),
635 doi:[10.1007/JHEP03\(2022\)197](https://doi.org/10.1007/JHEP03(2022)197), [2107.04561](https://doi.org/10.1093/acprof:oso/9780199238743.001.0001).
- 636 [16] K. Symanzik, *Renormalizable models with simple symmetry breaking. 1. Symmetry break-*
637 *ing by a source term*, Commun. Math. Phys. **16**, 48 (1970), doi:[10.1007/BF01645494](https://doi.org/10.1007/BF01645494).
- 638 [17] S. R. Coleman, R. Jackiw and H. D. Politzer, *Spontaneous Symmetry Breaking in the $O(N)$*
639 *Model for Large N^** , Phys. Rev. D **10**, 2491 (1974), doi:[10.1103/PhysRevD.10.2491](https://doi.org/10.1103/PhysRevD.10.2491).
- 640 [18] J. Iliopoulos, C. Itzykson and A. Martin, *Functional Methods and Perturbation Theory*,
641 Rev. Mod. Phys. **47**, 165 (1975), doi:[10.1103/RevModPhys.47.165](https://doi.org/10.1103/RevModPhys.47.165).
- 642 [19] R. W. Haymaker and J. Perez-Mercader, *Convexity of the Effective Potential*, Phys. Rev. D
643 **27**, 1948 (1983), doi:[10.1103/PhysRevD.27.1948](https://doi.org/10.1103/PhysRevD.27.1948).
- 644 [20] Y. Fujimoto, L. O’Raifeartaigh and G. Parravicini, *Effective Potential for Nonconvex Poten-*
645 *tials*, Nucl. Phys. B **212**, 268 (1983), doi:[10.1016/0550-3213\(83\)90305-X](https://doi.org/10.1016/0550-3213(83)90305-X).
- 646 [21] C. M. Bender and F. Cooper, *Failure of the Naive Loop Expansion for the Effective Potential*
647 *in ϕ^4 Field Theory When There Is ‘Broken Symmetry’*, Nucl. Phys. B **224**, 403 (1983),
648 doi:[10.1016/0550-3213\(83\)90383-8](https://doi.org/10.1016/0550-3213(83)90383-8).
- 649 [22] M. Hindmarsh and D. Johnston, *Convexity of the Effective Potential*, J. Phys. A **19**, 141
650 (1986), doi:[10.1088/0305-4470/19/1/016](https://doi.org/10.1088/0305-4470/19/1/016).

- 651 [23] J. Alexandre and A. Tsapalis, *Maxwell Construction for Scalar Field Theories*
652 *with Spontaneous Symmetry Breaking*, Phys. Rev. D **87**(2), 025028 (2013),
653 doi:[10.1103/PhysRevD.87.025028](https://doi.org/10.1103/PhysRevD.87.025028), [1211.0921](https://arxiv.org/abs/1211.0921).
- 654 [24] A. D. Plascencia and C. Tamarit, *Convexity, gauge-dependence and tunneling rates*, JHEP
655 **10**, 099 (2016), doi:[10.1007/JHEP10\(2016\)099](https://doi.org/10.1007/JHEP10(2016)099), [1510.07613](https://arxiv.org/abs/1510.07613).
- 656 [25] P. Millington and P. M. Saffin, *Visualising quantum effective action calculations in zero*
657 *dimensions*, J. Phys. A **52**(40), 405401 (2019), doi:[10.1088/1751-8121/ab37e6](https://doi.org/10.1088/1751-8121/ab37e6), [1905.](https://arxiv.org/abs/1905.09674)
658 [09674](https://arxiv.org/abs/1905.09674).
- 659 [26] V. A. Rubakov, *The Null Energy Condition and its violation*, Phys. Usp. **57**, 128 (2014),
660 doi:[10.3367/UFNe.0184.201402b.0137](https://doi.org/10.3367/UFNe.0184.201402b.0137), [1401.4024](https://arxiv.org/abs/1401.4024).
- 661 [27] D. A. Easson and J. E. Lesnefsky, *Eternal Universes* (2024), [2404.03016](https://arxiv.org/abs/2404.03016).
- 662 [28] V. Sopova and L. H. Ford, *The Energy density in the Casimir effect*, Phys. Rev. D **66**, 045026
663 (2002), doi:[10.1103/PhysRevD.66.045026](https://doi.org/10.1103/PhysRevD.66.045026), [quant-ph/0204125](https://arxiv.org/abs/quant-ph/0204125).
- 664 [29] N. Graham and K. D. Olum, *Negative energy densities in quantum field theory with a back-*
665 *ground potential*, Phys. Rev. D **67**, 085014 (2003), doi:[10.1103/PhysRevD.69.109901](https://doi.org/10.1103/PhysRevD.69.109901),
666 [Erratum: Phys.Rev.D 69, 109901 (2004)], [hep-th/0211244](https://arxiv.org/abs/hep-th/0211244).
- 667 [30] N. Graham and K. D. Olum, *Plate with a hole obeys the averaged null energy condition*,
668 Phys. Rev. D **72**, 025013 (2005), doi:[10.1103/PhysRevD.72.025013](https://doi.org/10.1103/PhysRevD.72.025013), [hep-th/0506136](https://arxiv.org/abs/hep-th/0506136).
- 669 [31] S. R. Coleman, *The Fate of the False Vacuum. 1. Semiclassical Theory*, Phys. Rev. D **15**,
670 2929 (1977), doi:[10.1103/PhysRevD.16.1248](https://doi.org/10.1103/PhysRevD.16.1248), [Erratum: Phys.Rev.D 16, 1248 (1977)].
- 671 [32] C. G. Callan, Jr. and S. R. Coleman, *The Fate of the False Vacuum. 2. First Quantum*
672 *Corrections*, Phys. Rev. D **16**, 1762 (1977), doi:[10.1103/PhysRevD.16.1762](https://doi.org/10.1103/PhysRevD.16.1762).
- 673 [33] H. Kleinert, *Path Integrals in Quantum Mechanics, Statistics, Polymer Physics, and Finan-*
674 *cial Markets*, doi:[10.1142/5057](https://doi.org/10.1142/5057) (2004).
- 675 [34] H.-T. Cho, J.-T. Hsiang and B.-L. Hu, *Quantum Capacity and Vacuum Compressibility of*
676 *Spacetime: Thermal Fields*, Universe **8**(5), 291 (2022), doi:[10.3390/universe8050291](https://doi.org/10.3390/universe8050291),
677 [2204.08634](https://arxiv.org/abs/2204.08634).
- 678 [35] I. H. Brevik, K. A. Milton and S. D. Odintsov, *Entropy bounds in $R \times S^{**3}$ geometries*,
679 Annals Phys. **302**, 120 (2002), doi:[10.1006/aphy.2002.6317](https://doi.org/10.1006/aphy.2002.6317), [hep-th/0202048](https://arxiv.org/abs/hep-th/0202048).
- 680 [36] C. G. Callan, S. B. Giddings, J. A. Harvey and A. Strominger, *Evanescent black holes*, Phys.
681 Rev. D **45**, R1005 (1992), doi:[10.1103/PhysRevD.45.R1005](https://doi.org/10.1103/PhysRevD.45.R1005).
- 682 [37] T. M. Fiola, J. Preskill, A. Strominger and S. P. Trivedi, *Black hole thermody-*
683 *namics and information loss in two-dimensions*, Phys. Rev. D **50**, 3987 (1994),
684 doi:[10.1103/PhysRevD.50.3987](https://doi.org/10.1103/PhysRevD.50.3987), [hep-th/9403137](https://arxiv.org/abs/hep-th/9403137).
- 685 [38] J. G. Russo, L. Susskind and L. Thorlacius, *End point of hawking radiation*, Phys. Rev. D
686 **46**, 3444 (1992), doi:[10.1103/PhysRevD.46.3444](https://doi.org/10.1103/PhysRevD.46.3444).
- 687 [39] S. Bose, L. Parker and Y. Peleg, *Semiinfinite throat as the end state geome-*
688 *try of two-dimensional black hole evaporation*, Phys. Rev. D **52**, 3512 (1995),
689 doi:[10.1103/PhysRevD.52.3512](https://doi.org/10.1103/PhysRevD.52.3512), [hep-th/9502098](https://arxiv.org/abs/hep-th/9502098).

- 690 [40] J. Cruz and J. Navarro-Salas, *Solvable models for radiating black holes and area preserving*
691 *diffeomorphisms*, Phys. Lett. B **375**, 47 (1996), doi:[10.1016/0370-2693\(96\)00246-8](https://doi.org/10.1016/0370-2693(96)00246-8),
692 [hep-th/9512187](https://arxiv.org/abs/hep-th/9512187).
- 693 [41] R. Jackiw, *Lower Dimensional Gravity*, Nucl. Phys. B **252**, 343 (1985), doi:[10.1016/0550-3213\(85\)90448-1](https://doi.org/10.1016/0550-3213(85)90448-1).
- 695 [42] D. Grumiller, W. Kummer and D. V. Vassilevich, *Dilaton gravity in two-dimensions*, Phys.
696 Rept. **369**, 327 (2002), doi:[10.1016/S0370-1573\(02\)00267-3](https://doi.org/10.1016/S0370-1573(02)00267-3), [hep-th/0204253](https://arxiv.org/abs/hep-th/0204253).
- 697 [43] A. Fabbri and J. Navarro-Salas, *Modeling black hole evaporation*, Imperial College Press-
698 World Scientific, London (2005).
- 699 [44] S. Djordjević, A. Gočanin, D. Gočanin and V. Radovanović, *Page curve for an eternal*
700 *Schwarzschild black hole in a dimensionally reduced model of dilaton gravity*, Phys. Rev. D
701 **106**(10), 105015 (2022), doi:[10.1103/PhysRevD.106.105015](https://doi.org/10.1103/PhysRevD.106.105015), [2207.07409](https://arxiv.org/abs/2207.07409).
- 702 [45] S. B. Giddings and A. Strominger, *Dynamics of extremal black holes*, Phys. Rev. D **46**, 627
703 (1992), doi:[10.1103/PhysRevD.46.627](https://doi.org/10.1103/PhysRevD.46.627), [hep-th/9202004](https://arxiv.org/abs/hep-th/9202004).
- 704 [46] A. Strominger, *Faddeev-Popov ghosts and (1+1)-dimensional black hole evaporation*, Phys.
705 Rev. D **46**, 4396 (1992), doi:[10.1103/PhysRevD.46.4396](https://doi.org/10.1103/PhysRevD.46.4396), [hep-th/9205028](https://arxiv.org/abs/hep-th/9205028).
- 706 [47] J. A. Harvey and A. Strominger, *Quantum aspects of black holes*, In *Spring School on*
707 *String Theory and Quantum Gravity (To be followed by Workshop on String Theory 8-10*
708 *Apr)*, pp. 175–223 (1993), [hep-th/9209055](https://arxiv.org/abs/hep-th/9209055).
- 709 [48] A. R. Mikovic and V. Radovanovic, *One loop effective action for a generic 2-D dilaton*
710 *gravity theory*, Nucl. Phys. B **504**, 511 (1997), doi:[10.1016/S0550-3213\(97\)00474-4](https://doi.org/10.1016/S0550-3213(97)00474-4),
711 [hep-th/9704014](https://arxiv.org/abs/hep-th/9704014).
- 712 [49] S. M. Christensen and S. A. Fulling, *Trace anomalies and the hawking effect*, Phys. Rev. D
713 **15**, 2088 (1977), doi:[10.1103/PhysRevD.15.2088](https://doi.org/10.1103/PhysRevD.15.2088).
- 714 [50] R. C. Myers, *Black hole entropy in two-dimensions*, Phys. Rev. D **50**, 6412 (1994),
715 doi:[10.1103/PhysRevD.50.6412](https://doi.org/10.1103/PhysRevD.50.6412), [hep-th/9405162](https://arxiv.org/abs/hep-th/9405162).
- 716 [51] S. Hirano, *Island formula from Wald-like entropy with backreaction*, JHEP **02**, 125 (2024),
717 doi:[10.1007/JHEP02\(2024\)125](https://doi.org/10.1007/JHEP02(2024)125), [2310.03416](https://arxiv.org/abs/2310.03416).
- 718 [52] V. Iyer and R. M. Wald, *Some properties of the noether charge and a proposal for dynamical*
719 *black hole entropy*, Phys. Rev. D **50**, 846 (1994), doi:[10.1103/PhysRevD.50.846](https://doi.org/10.1103/PhysRevD.50.846).
- 720 [53] M.-H. Yu and X.-H. Ge, *Entanglement islands in generalized two-dimensional dilaton black*
721 *holes*, Phys. Rev. D **107**(6), 066020 (2023), doi:[10.1103/PhysRevD.107.066020](https://doi.org/10.1103/PhysRevD.107.066020), [2208.](https://arxiv.org/abs/2208.01943)
722 [01943](https://arxiv.org/abs/2208.01943).
- 723 [54] J. F. Pedraza, A. Svesko, W. Sybesma and M. R. Visser, *Semi-classical thermodynam-*
724 *ics of quantum extremal surfaces in Jackiw-Teitelboim gravity*, JHEP **12**, 134 (2021),
725 doi:[10.1007/JHEP12\(2021\)134](https://doi.org/10.1007/JHEP12(2021)134), [2107.10358](https://arxiv.org/abs/2107.10358).
- 726 [55] J. D. Hayward, *Entropy in the RST model*, Phys. Rev. D **52**, 2239 (1995),
727 doi:[10.1103/PhysRevD.52.2239](https://doi.org/10.1103/PhysRevD.52.2239), [gr-qc/9412065](https://arxiv.org/abs/gr-qc/9412065).
- 728 [56] M. Visser, *Gravitational vacuum polarization. 3: Energy conditions in*
729 *the (1+1) Schwarzschild space-time*, Phys. Rev. D **54**, 5123 (1996),
730 doi:[10.1103/PhysRevD.54.5123](https://doi.org/10.1103/PhysRevD.54.5123), [gr-qc/9604009](https://arxiv.org/abs/gr-qc/9604009).

- 731 [57] A. Widom, E. Sassaroli, Y. N. Srivastava and J. Swain, *The Casimir effect and thermody-*
732 *namic instability* (1998), [quant-ph/9803013](#).
- 733 [58] E. Sassaroli, Y. N. Srivastava, J. Swain and A. Widom, *The Dynamical and static Casimir*
734 *effects and the thermodynamic instability*, In *ITAMP Topical Group on Casimir Forces Atomic*
735 *and molecular physics*. (1998), [hep-ph/9805479](#).
- 736 [59] J. Alexandre and D. Backhouse, *Tunnelling and the Casimir effect on a D-dimensional*
737 *sphere* (2024), [2408.17189](#).
- 738 [60] M. K. Parikh and F. Wilczek, *Hawking radiation as tunneling*, *Physical Review Letters*
739 **85**(24), 5042 (2000), doi:[10.1103/physrevlett.85.5042](#).